Nonhydrogen isotope effects on structural phase transitions in dielectric crystals

T. Hidaka and K. Oka
Electrotechnical Laboratory, 1-1-4 Umezono, Tsukuba-shi, Ibaraki-ken 305, Japan
(Received 23 March 1990; revised manuscript received 9 July 1990)

The effect of isotope substitutions on the phase-transition temperatures in $LiTaO_3$ (Li), $PbZrO_3$ (Zr), KH_2PO_4 (K and O), $NH_4H_2PO_4$ (N), K_2SeO_4 (O), Rb_2ZnCl_4 (Rb and Zn), $NaNO_2$ (N), and KNO_3 (N) are given. Parentheses denote atoms for which isotopes have been substituted. Except for $NaNO_2$, all of the materials studied show higher phase-transition temperatures when *lighter* isotopes are substituted, and vice versa for heavier isotopes. This is opposite to the effect of deuteron substitution in potassium dihydrogen phosphate (KDP)-type crystals. The results suggest that the role of the ionic masses for atoms heavier than hydrogen differs completely from the role of hydrogen. $NaNO_2$ scarcely showed any isotope effect despite heavy ^{15}N substitution; this suggests that $NaNO_2$ undergoes a pure Weiss-type order-disorder phase transition due to rigid permanent dipoles on NO_2^-, whereas the other materials cannot be described by the simplest Weiss model.

I. INTRODUCTION

The H-D isotope effects in KDP (KH_2PO_4) type crystals (with hydrogen bond) are well known in solid-state physics.[1] With deuteron (D) introduction, the ferroelectric phase transition temperature, T_c, of KDP rises remarkably. The correct treatment of the effect may be essential for the theory of KDP. Also, we can suppose that other atoms in KDP-type crystals must exhibit the isotope effect. Since, from the viewpoint of classical thermostatistical theory, heavy isotopes should have weaker thermodynamic fluctuation than light isotopes at the same temperature, we can expect that materials with heavy isotopes should have higher transition temperatures than those with light isotopes. It is important to check the isotope effect behind the hydrogen isotope effect. However, to our knowledge no report has been published concerning isotope effects except for hydrogen, not only for KDP-type crystals but also for crystals without hydrogen bonds, such as $BaTiO_3$.

Recently, the Ba and Ti isotope effects on T_c in $BaTiO_3$ have been reported.[2] A remarkable fact was that with the introduction of *light* isotopes (^{46}Ti or ^{134}Ba), T_c *rose* sharply, and vice versa for heavy ^{50}Ti. The trend of the isotope-mass-exchange effect in $BaTiO_3$ is the *opposite* of the isotope effect in KDP-type crystals for deuteron introduction, and is contrary to the prediction of classical thermostatistics. We suppose that the influence of the isotope mass in $BaTiO_3$ on its phase transition differs from the hydrogen mass in hydrogen-bonded KDP-type crystals. Also, we should reconsider the applicability of the classical thermostatistics for the structural phase transition. However, to date, no other data exist for isotope substitutions except for $BaTiO_3$. We cannot deny the possibility that the observed isotope effect in $BaTiO_3$ was due to spurious chemical impurities. Thus, it is strongly desirable to study other isotope effects behind $BaTiO_3$.

We report here the effects of isotope substitution on the structural phase transitions of the following: $\underline{Li}TaO_3$, $PbZrO_3$, $\underline{K}H_2PO_4$, $\underline{N}H_4H_2PO_4$, K_2SeO_4, Rb_2ZnCl_4, $NaNO_2$, and KNO_3, all for the first time. Underlined elements are those for which we have studied the isotope effects.

The first crystal, $LiTaO_3$, is one of the Γ-point (Brillouin zone center) ferroelectric phonon freezing materials, as is $BaTiO_3$, with T_c of 665 °C.[3] But the phase transition in $LiTaO_3$ is *second order,* whereas that in $BaTiO_3$ is *first order.* It is interesting to know whether or not the second-order phase transition shows the same isotope effect as the first-order one.

The next one, $PbZrO_3$, shows a *zone-boundary* phonon freezing (antiferroelectric) phase transition at about 230 °C (T_a: T_a means the antiferroelectric phase transition temperature).[4] The hydrostatic-pressure dependence of the zone-boundary phonon-type phase transitions is opposite to that of the zone-center phonon phase transitions.[5] The softening mechanism of the zone-boundary phonon phase transitions is supposed to be somewhat different to that of the zone-center phonon-type phase transitions, from the viewpoint of the pressure dependence. It remains a possibility that the zone-boundary phonon-type transitions have the opposite isotope effect from that obtained in the zone-center-type phase transitions.

KH_2PO_4 (KDP) and $NH_4H_2PO_4$ (ADP) are representative hydrogen-bonded crystals showing ferroelectric and antiferroelectric phase transitions, respectively. We have a strong interest in the isotope effect in these crystals for ions heavier than hydrogen. We report the isotope effects for K and O in KDP, and the effect for N isotope substitution in ADP.

K_2SeO_4 and its isomorphic Rb_2ZnCl_4 show *incommensurate* phase transitions of the *first kind* at about −145 °C and 29 °C, respectively.[6–8] The incommensurate-type phonon freezing seems to interpolate between the two cases of transitions; zone-center phonon freezing and zone-boundary phonon freezing. It is interesting to

know the isotope effects in them, compared with zone-center-type or zone-boundary-type phase transitions.

$NaNO_2$ is one of the crystals that shows incommensurate-type phase transitions of the *second kind*.[8-10] It is important to study the isotope effects on the incommensurate phase transitions of the second kind, for comparison with the incommensurate phase transition of the first kind such as in K_2SeO_4. $NaNO_2$ is called the molecular-type crystals. The term "molecular-type crystal" means that it will be decomposed into Na^+ and NO_2^- molecules by heating. NO_2^- is an ionic molecule with a *permanent dipole*. Such a situation differs fundamentally from other materials described above. For example, KH_2PO_4 will be decomposed into K^+, H^+, and PO_4^{3-} by heating, whereas PO_4^{3-} does *not* have a permanent dipole in its molecular state (cubic tetrahedron). Therefore, the difference between the isotope effect in $NaNO_2$ (with microscopic permanent dipole) and those in other crystals (without permanent dipole) is likely to be very interesting. KNO_3 is also a molecular crystal without a permanent dipole.[11,12] Therefore, we can suppose that the isotope effect in KNO_3 may be somewhat different from $NaNO_2$. It is important to study the isotope effect in KNO_3 for comparison with $NaNO_2$.

II. EXPERIMENTAL

In this section we report the isotope effects in detail. We mainly used the differential scanning calorimetric (DSC) method to define the phase transition temperatures of respective materials. The DSC method is useful for determining the phase transition temperatures.[13,14] The principle of the DSC method is as follows: The sample under test (by an amount of 1 to 100 mg) is heated to raise its temperature at a constant rate from a temperature lower than T_c to a temperature higher than T_c. The sample has its own heat capacity; the rising of the sample temperature delays somewhat from the thermal-bath temperature. To compensate for this temperature difference between the sample and the thermal bath, we add excess thermal energy to the sample. The added excess thermal energy (which is recorded as the DSC signal) is proportional to the heat capacity (c_p) of the sample. At the phase transition, the c_p of the material changes abruptly; we can determine T_c from the abrupt change in DSC data (which should correspond exactly to the change in the c_p). The DSC method is applicable for most of all types of phase transitions. On the contrary, methods such as the measurement of dielectric-capacitance is applicable only for materials that show large dielectric-constant anomalies at their phase transitions.

There are two types of phase transitions in dielectric materials. One is the so called first-order type ($BaTiO_3$, etc.), and the other, the second-order type ($LiTaO_3$, etc.). In the first-order transition with a δ-function-type specific heat anomaly (a latent heat) at T_c, the DSC signal (which in this case is the excess thermal flow needed to compensate the latent heat) starts just at T_c. Thus, we can define T_c to be equal to the onset temperature of the DSC signal. In second-order phase transitions, however, the specific heat is λ type which means that the DSC signal has a long tail for temperatures much lower than T_c (for example in $LiTaO_3$ the specific heat anomaly trails until 200 °C lower than T_c).[15] It is very difficult to define the onset temperatures for second-order phase transitions. Under suitable conditions (a satisfactorily slow rate of increase of temperature, a small sample, and good thermal conductivity between sample and the thermal bath), the temperature where the peak in the DSC signal gives T_c for second-order transitions more than the onset temperature does. In this paper, we therefore determine T_c for the second-order phase transition materials from the temperature of the peak in the DSC signals rather than the onset temperatures. In ferroelectric materials with first-order phase transitions such as $BaTiO_3$, their c_p have also long tails well below T_c, in contrast with the solid-liquid transitions (pure first order). In the case of $BaTiO_3$, the tail extends about 10 °C,[14,16] because the long-range ordering still grows up for 10 °C lower temperature than T_c. As a result, the onset temperatures in the DSC signals for the first-order-transition ferroelectric materials are not clear, as was in the second-order-transition materials. It is therefore desirable to use the peak-DSC-signals temperature to define T_c in these first-order-transition materials, as well. It is then expected that T_c defined from the peak in the DSC signals will be somewhat higher than the exact T_c. However, we do not need the exact T_c, but only the isotope shift. With the same experimental conditions in the DSC measurements for respective isotope enriched materials, we can get accurate shifts of T_c.

Both the transition heat, ΔQ, and the specific heat, c_p, can be obtained from DSC measurements. However, the data (ΔQ_p or c_p), deduced from the DSC data may include some ambiguity ($\pm 20\%$ or more) because of heat leak, base line drift, etc., in the DSC measurements. Also, for absolute ΔQ or c_p, we need to calibrate the sensitivities of the DSC equipment used for respective materials, because of the different thermal capacities and thermal conductivities in respective materials. This is very troublesome and, for our purpose (to determine the isotope effects in T_c), is not needed. We will give only relative transition heat, ΔQ, at the phase transitions of respective isotope enriched materials, in comparison with the reference materials including naturally obtained isotopes.

Thermal measurements were done with Rigaku model DSC-8400, Seiko model DSC-200, and Mettler model DSC-30 meter. For several materials such as K_2SeO_4, we checked for systematic error between those equipments for reliability of the DSC data, because of small isotope effects and weak DSC signals in these materials. The weights of the samples measured and the rate of temperature increase (and decrease) for the DSC measurements were selected to obtain best data for each material. The best conditions for each sample will be presented in respective subsection. Of course, for reference materials with natural isotopes, the sample weight was selected to

be equal to that of the corresponding isotope enriched material, and the temperature scanning rates for them were also set equal. The resolution of the isotope shift, $\Delta T_c/T_c$, was of the order of 0.15–0.2 % in three apparatuses used. The resolution was checked using $(NH_4)_2SO_4$ and $(ND_4)_2SO_4$. $(ND_4)_2SO_4$ has T_c which is about 0.5 °C higher than $(NH_4)_2SO_4$;[17] making this very convenient to test the resolution.

For $PbZrO_3$ we used not only the DSC method but also the capacitance measurement methods to determine phase transition temperature. The reason will be given in Sec. II B.

A. $LiTaO_3$

Normal $LiTaO_3$ (mainly includes ^7Li) has a ferroelectric phase transition temperature, T_c, of 665 °C (Ref. 3). ^6Li and ^7Li isotope substitutions for natural Li (its atomic mass is 6.94) may give a large effect on T_c, because the mass shift in the reduced mass, μ_{TO}, of the Γ-point transverse optical phonon is large. μ_{TO} may be given by, for simplicity

$$1/\mu_{TO}=1/\mu_{Li}+1/3\mu_O\ , \tag{1}$$

where μ_{Li} and μ_O are the atomic masses of Li and O, respectively. Here we ignored the mass of Ta because of its weight (180.95 in atomic units). The relative shift of μ_{TO} from ^6Li to ^7Li is 14.5%. It is 3 times larger than that produced by replacement of ^{50}Ti for ^{46}Ti in $BaTiO_3$ (about 4%). Therefore, the Li isotope effect is expected to be very large in $LiTaO_3$.

99.16% ^6Li-enriched $LiOH:H_2O$ powder and 99.99% ^7Li-enriched $LiOH:H_2O$ powder were supplied by the Oak Ridge National Laboratory (Lot No. are 41-1079 and 41-1080, respectively). Two powders, one with $^6LiOH:H_2O$ and stoichiometric Ta_2O_3, and the other with $^7LiOH:H_2O$ and stoichiometric Ta_2O_3, were heated up to 1000 °C for 5 h (first firing). Next, we pressed them into 12-mm-diameter and 1-mm-thick pellets, then heated up to 1400 °C for 5 h (second firing). Throughout the thermal treatments, the two samples were kept together in a crucible, but separated by a Pt sheet. This was done to keep the firing conditions for both samples as identical as possible. We obtained hard and white ceramics. The T_c of them were determined by the DSC measurement. Figure 1 shows the DSC data of $^6LiTaO_3$ and $^7LiTaO_3$ (for heating procedures). The masses of the samples of the DSC measurements were about 100 mg, and the temperature rising rate was 20 °C/min. In $LiTaO_3$, the specific heat anomaly trails much lower than T_c (until about 400 °C).[15] Thus, we could not show the onset temperatures of the DSC signals in Fig. 1. The peak DSC signal temperature for $^6LiTaO_3$ was 667.5 °C, and that of $^7LiTaO_3$ was 655.9 °C. Also, the ending temperatures (for heating procedures) of the DSC data were 687.8 °C and 669.5 °C, respectively. The ending temperatures were defined to be the refracting points on the DSC signals in Fig. 1. The reproducibility of the DSC data was enough to determine the peak and ending temperatures within 2 °C. The peak and ending temperatures in $^6LiTaO_3$ were

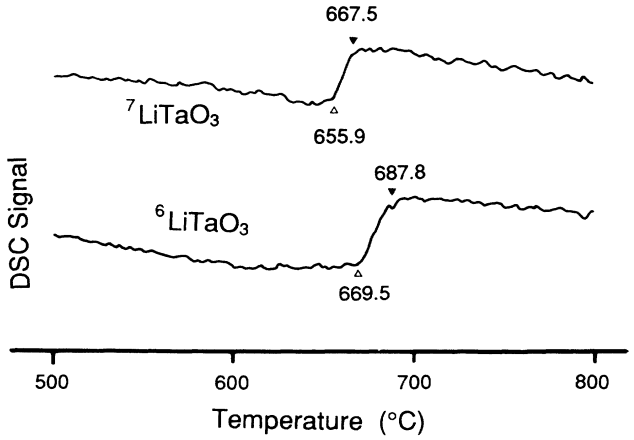

FIG. 1. DSC signals of $^6LiTaO_3$ and $^7LiTaO_3$ (on heating). The light $^6LiTaO_3$ seems to have a 15–20 °C higher transition temperature than heavy $^7LiTaO_3$. The apparatus was a Seiko model DSC-200. The DSC signals trail far below T_c. Therefore, the DSC-signal-onset temperatures are not shown. The DSC signal of the crystal with light Li isotope is 1.2 times stronger than that for the crystal with heavy Li isotope.

15–20 °C higher $^7LiTaO_3$. Thus, we can conclude that the sample with the light ^6Li isotope has 15–20 °C higher T_c than the one with heavier ^7Li. The isotope shift is large enough to be distinguished from shift due to chemical impurities. The trend in the Li isotope effect on $LiTaO_3$ is the same as in $BaTiO_3$. The difference in the DSC signals of $^6LiTaO_3$ and $^7LiTaO_3$ is large enough to determine the isotope effect of Li without the need for capacitance measurements. Natural $LiTaO_3$, including natural Li (mixture of ^6Li and ^7Li) with an atomic mass of 6.94, has a T_c of about 665 °C. This T_c (665 °C) lies between those of $^7LiTaO_3$ and $^6LiTaO_3$ obtained in this paper. Thus, the results for $^7LiTaO_3$ and $^6LiTaO_3$ are very reasonable. The total transition heats, ΔQ, for $^6LiTaO_3$ and $^7LiTaO_3$ relative to the referenced sample with naturally obtained isotopes are given in Table III, together with the isotope shift in T_c. We give, hereafter, relative ΔQ of respective materials only in Table III. The ΔQ of heavy-^7Li-enriched $LiTaO_3$ is 1.2 times larger than that of $^6LiTaO_3$.

B. $PbZrO_3$

As noted in the Introduction, $PbZrO_3$ shows an interesting *antiferroelectric* phase transition at about 230 °C (T_a).[4] The high temperature structure is cubic, the same as $BaTiO_3$. However, the structure below 230 °C is antiferroelectric (space group is *Pbam*). The fictitious ferroelectric Curie temperature, T_c, which is defined as the divergence temperature of dielectric constant extrapolated from the high temperature (paraelectric) region, is just slightly less than T_a. Thus, we suppose that the mechanisms responsible for freezing out these two phonons (zone center and zone boundary) are related together in $PbZrO_3$. The isotope effect on the antiferroelectric phase transition is very interesting.

Powders of ^{90}Zr- and ^{94}Zr-enriched ZrO_2 were supplied

by the Oak Ridge National Laboratory. Their lot Nos. are 188801 and 189101, respectively. Their isotope contents are given in Table I. Two powders, one with $^{90}ZrO_2$ mainly and stoichiometric PbO, and the other with $^{94}ZrO_2$ mainly and stoichiometric PbO, were heated up to 800 °C for 4 h (first firing). The two kinds of powders obtained were pressed into the form of 12 mm in diameter and 1 mm in thick pellets, and heated up to 1200 °C for 1 h (second firing). During these firings, the samples were immersed in a PbO-vapor-enriched atmosphere, because PbO in $PbZrO_3$ is very volatile. The two samples were kept together in a crucible, separated by a Pt sheet throughout the thermal treatments.

The DSC signals for $Pb^{90}ZrO_3$ and $Pb^{94}ZrO_3$ are shown in Fig. 2, for heating procedure. The masses of measured samples were about 20 mg and the rate of temperature increase was 10 °C/min. We observed a relatively weak isotope effect for $PbZrO_3$; however, qualitatively speaking, it seems to be in agreement with the isotope effects in $BaTiO_3$ and $LiTaO_3$. With light isotope (^{90}Zr) introduction, T_a rises, and vice versa. Also, the measured ΔQ for both samples were equal, within experimental error.

The DSC data did not give us a clear isotope effect. Fortunately, we could produce good sintered pellets by the above method suitable for capacitance measurements. The dielectric constants of the $Pb^{90}ZrO_3$ and $Pb^{94}ZrO_3$ are shown in Fig. 3, which were measured with an automatic capacitance meter at 10 kHz. We see, from Fig. 3, that the light (^{90}Zr)-enriched $PbZrO_3$ has the higher T_a than the heavy (^{94}Zr)-enriched one by an amount of 4 °C. The accuracy in defining T_a was about 1 °C. The Zr isotope effect in $PbZrO_3$ is somewhat weaker than that of T_c in $LiTaO_3$ or $BaTiO_3$. The result is quite reasonable. In $PbZrO_3$, Pb atoms move mainly with the phase transition from their equilibrium positions at the higher temperature phase. The shift of Zr atoms is smaller than that of Ti in $BaTiO_3$, or Li in $LiTaO_3$. Therefore, the lattice dynamical weight of Zr in the eigenvector of the phonon relating to the phase transition is small. Our weak Zr-isotope effect obtained in this paper is consistent with such a situation.

C. KDP and ADP

KDP (KH_2PO_4) and ADP ($NH_4H_2PO_4$) are, respectively, famous ferroelectric and antiferroelectric crystals with hydrogen bonds. They exhibit large hydrogen-isotope effects on their phase transitions.[1] However, to our knowledge, there are no reports concerning the isotope effects of ions, other than hydrogen, such as oxygen. With the phase transition in KDP, the relative positions of K, P, and O are shifted. Therefore, we can expect K and O isotope effects on the phase transition. For P, there is no stable isotope other than ^{31}P. We studied the ^{39}K-^{41}K and ^{16}O-^{18}O isotope effects in KDP. Also, we studied the ^{14}N-^{15}N isotope effect in ADP.

TABLE I. Isotope contents in ^{90}Zr-enriched and ^{94}Zr-enriched two kinds of ZrO_2 powders, A and B, supplied by the Oak Ridge National Laboratory.

Sample	Isotope contents (%) ^{90}Zr	^{91}Zr	^{92}Zr	^{94}Zr	^{96}Zr
A(^{90}Zr enriched)	99.36	0.30	0.17	0.12	0.04
B(^{94}Zr enriched)	0.71	0.21	0.38	98.58	0.12

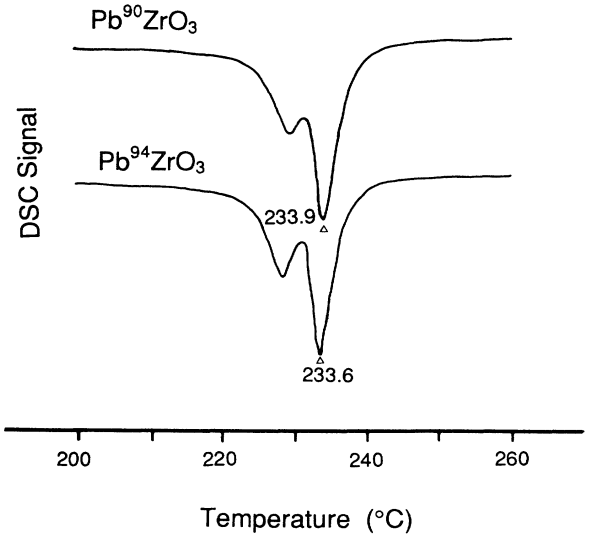

FIG. 2. DSC signals of $Pb^{90}ZrO_3$ and $Pb^{94}ZrO_3$ (on heating). The apparatus was a Seiko model DSC-200. We observed very weak isotope effect.

The method to fabricate ^{18}O-enriched KDP is as follows: The mixture of KCl (for example, 50 mg) and stoichiometric (139.65 mg) PCl_5 was dissolved into 1 g of $H_2{}^{18}O$. ^{18}O-enriched water, with 98.8 atomic % ^{18}O, was supplied by ISOTEC Inc. (lot No. N50953). Next we distilled off HCl and excess $H_2{}^{18}O$ by heating up to 90 °C, and obtained a 100 mg of polycrystal of KDP. We also

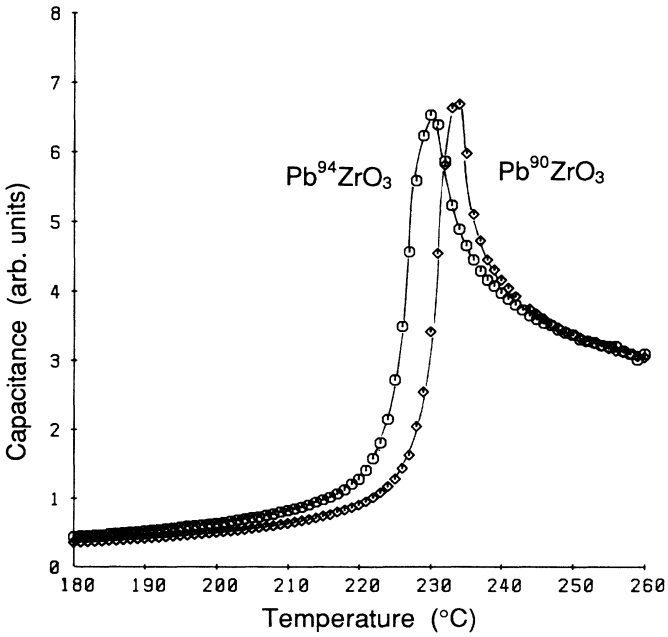

FIG. 3. Dielectric capacitances (normalized to 25 °C values, respectively) of $Pb^{90}ZrO_3$ and $Pb^{94}ZrO_3$ (on heating). About 4 °C difference was observed between the peaks.

fabricated a reference sample using natural water ($H_2{}^{16}O$), according with the same procedure shown above. Also, for the heavy ^{41}K introduced sample, we used 98.88% ^{41}K-enriched KCl, supplied by ISOTEC Inc. (Lot No. NS-0644), as the starting material in the above procedure. The degree of ^{18}O and ^{41}K enrichment in synthesized KDP using the above procedure is presumed to be the same as the degree of enrichment in the original materials ($H_2{}^{18}O$ and ^{41}KCl).

We measured the T_c for all crystals using the DSC method. Figure 4 shows the DSC signals (all for heating procedures). The masses of the samples to be measured were all about 20 mg, and the rate of temperature increase was 2 °C/min. The phase transition temperatures were defined from the peaks of the DSC signals. The samples enriched with heavy isotopes (^{18}O and ^{41}K) show a lower T_c than natural KDP with ^{16}O and ^{39}K. The reproducibility of the peak temperature in the DSC signals was better than 0.3 °C. The relative ΔQ of them are given in Table III.

A 96% ^{15}N-enriched ADP was supplied by CEA Co., France (Lot No. 83152). The degree of ^{15}N enrichment was confirmed by infrared absorption spectroscopy for N-H vibration frequency, to be in good agreement with the nominal value (more than 95%). Two ADP powders, one with ^{15}N and the other with ^{14}N (reference) were recrystallized once by an aqueous solution method. Figure 5 shows the DSC signals of the two kinds of ADP, for heating procedure. The masses to be measured were all 10 mg, and the rate of temperature rising was 10 °C/min. The heavy ^{15}N-enriched ADP showed about 1.2 °C lower T_a than natural ADP (with 99.6% ^{14}N). The reproducibility of the peak temperature in the DSC data was about 0.2 °C. The trend of the heavy-element isotope effects in KDP and ADP are opposite to that of the H-D isotope effects in them.

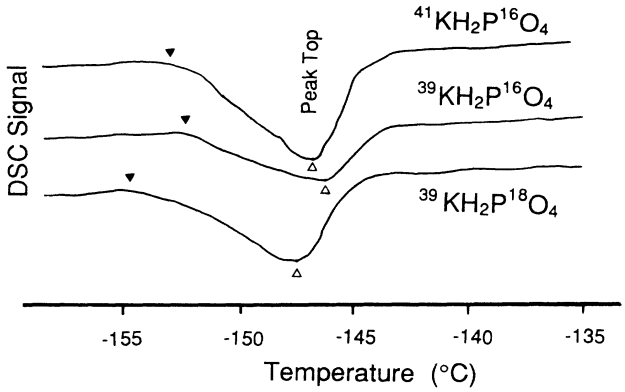

FIG. 4. DSC signals of three types of KDP: $^{39}KH_2P^{16}O_4$ (reference), $^{41}KH_2P^{16}O_4$, and $^{39}KH_2P^{18}O_4$ (on heating). We defined the peak temperature in the DSC signal as the phase transition temperature, T_c. In heavy ^{41}K- and ^{18}O-enriched KDP, T_c lowers from natural (^{39}K and ^{16}O including) KDP, by an amount of 0.5 °C and 1 °C, respectively. The apparatus used to obtain these data was a Rigaku model DSC-8430. The onset temperatures of heavy isotope- (^{41}K or ^{18}O) enriched materials seemed to be 1 °C and 2 °C lower than the natural one (^{39}K and ^{16}O), respectively.

D. K_2SeO_4 and Rb_2ZnCl_4

K_2SeO_4 and its isomorphic Rb_2ZnCl_4 show incommensurate phase transitions at −145 °C and 29 °C (T_i), respectively.[6,7] The incommensurate phase transitions in them are of the *first kind*.[8] The incommensurate phase transition has been thought to give interpolating data between two types of the transitions, zone-center phonon-freezing-type and zone-boundary phonon-freezing-type phase transitions. Thus, the isotope effect on the incommensurate phase transitions will give the interpolating data on those two phase transitions. It is very important to study the isotope effects on incommensurate phase transitions.

Commercially available K_2SeO_4 was recrystallized twice from an aqueous solution. The 100 mg of the recrystallized K_2SeO_4 was dissolved into 1 g of ^{18}O-enriched (by an amount of 98.8% in atomic weight, supplied by ISOTEC Inc.) water. Also, another 100 mg of the K_2SeO_4 was dissolved into 1 g of natural water, for the reference material. Two solutions with $H_2{}^{18}O$ and $H_2{}^{16}O$, respectively, were sealed in separate silica tubes, and heated up to 270 °C for 10 h to exchange ^{16}O in the original K_2SeO_4 with ^{18}O in $H_2{}^{18}O$. After this thermal treatment, the silica tubes were opened and recrystallized once more by an evaporation method. In 100 mg of original K_2SeO_4, about 29 mg of ^{16}O is included. 1 g of $H_2{}^{18}O$ includes about 900 mg of ^{18}O. Thus, in the sealed tube, 96% of all oxygen atoms were ^{18}O. Therefore, when the O in $H_2{}^{18}O$ and O in K_2SeO_4 reach into equilibrium by heating, then we can expect that K_2SeO_4 in the tube will have more than 95% of ^{18}O. The oxygen enrichment degree was determined by an infrared absorption measurement. Figure 6 shows the infrared absorption data of the two samples. One is the original (reference) with ^{16}O and the other ^{18}O enriched by the above method. The apparatus used was a Hitachi IR-260-50 double-flux spectrophotometer, and we used the so-called KBr powder method. From the vibration frequencies of two samples around 850 cm^{-1} (ν_3-F_2 mode of $SeO_4{}^{2-}$)

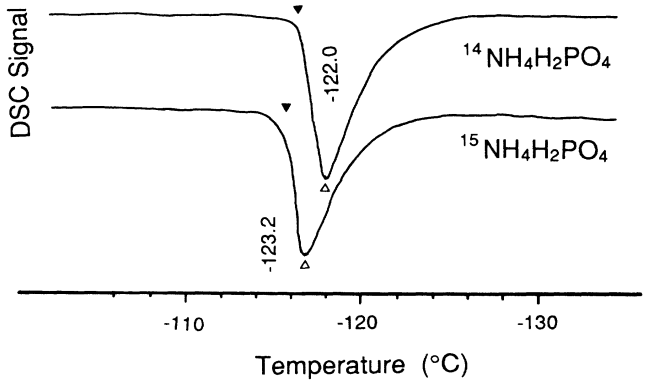

FIG. 5. DSC signals of $^{15}NH_4H_2PO_4$ and $^{14}NH_4H_2PO_4$ (reference). Heavy ^{15}N-enriched ADP shows about 1.2 °C lower T_a than natural (^{14}N-enriched) ADP. The apparatus was a Rigaku model DSC-8430. The onset temperature of heavy (^{15}N) isotope-enriched ADP was 1 °C lower than light (natural) ADP.

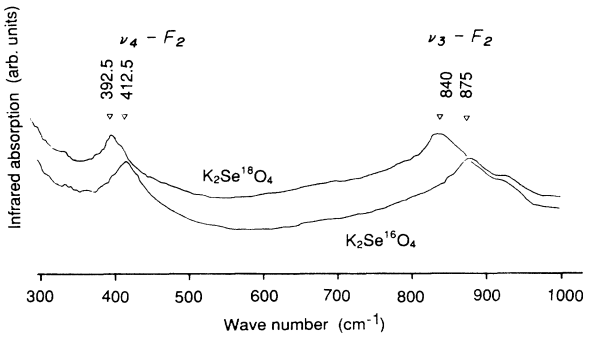

FIG. 6. Infrared absorption spectra of $K_2Se^{18}O_4$ and $K_2Se^{16}O_4$ (reference). Two Se—O vibration frequencies (ν_3-F_2 and ν_4-F_2) are lowered with ^{18}O introduction. From those frequency shifts at around 850 cm^{-1} and 400 cm^{-1}, we estimated the content of ^{18}O to be better than 95%.

and around 400 cm^{-1} (ν_4-F_2 mode), we estimated the ^{18}O enrichment degree of the sample. The ν_3-F_2 vibration mode of SeO_4^{2-} tetrahedron in K_2SeO_4 is shown in Fig. 7, schematically. Central Se moves, for example, in the positive z direction and the four O moves in the negative z direction in the ν_3 mode; hence the reproduced mass, $\mu_3(\nu_3)$, of the mode is given as

$$\mu_3(\nu_3)=1/\{1/\mu_{Se}+1/(4\mu_O)\} , \quad (2)$$

where μ_{Se} is the mass of Se and μ_O is that of O. μ_{Se} is 79 in atomic unit; thus

$$\mu_3(^{16}O)=35.35, \quad \mu_3(^{18}O)=37.67 , \quad (3)$$

where $\mu_3(^{16}O)$ means the reduced mass for ^{16}O, and so on. The vibration frequency, $\omega(\mu_3)$, is proportional to the inverse square root of μ_3. The expected frequency ratio for ^{16}O sample to ^{18}O fully enriched sample is then 1.0323, from Eq. (3). Figure 6 gives the experimental ratio of ν_3-vibration frequencies of them, to be 1.04±0.005; somewhat larger than the calculated one. This difference between the experimental and calculated values is reasonable because we ignored the weight of K ions in K_2SeO_4. In K_2SeO_4, K and Se cations may move together, because Se^{6+} has large amount of positive charge; Se and K form a rigid skeleton network, and in the network O_4^{8-} clusters move in an opposite direction from the cations (K^+ and Se^{6+}). We should therefore change μ_{Se} in Eq. (3) to $\mu_{Se}+2\mu_K$. From the correction we obtained a reasonable frequency ratio, 1.042, between the material with ^{16}O to a theoretical material with 100% ^{18}O, for ν_3-F_2 mode. The experimental value was 1.04 (including the experimental error of order 0.005), in agreement with the expected value. We, therefore, believe that the ^{18}O-enriched material includes more than 95% of ^{18}O. The estimation of ^{18}O enrichment degree from the ν_4-F_2 mode was in good agreement with the value determined from the ν_3-F_2 mode.

Figure 8 shows the DSC data of those two samples. The weights of these samples measured were 16 mg and the temperature rising rate was 5 °C/min. The heavy ^{18}O-enriched sample ($K_2Se^{18}O_4$) shows about 2.4 °C lower T_i than the natural isotope sample ($K_2Se^{16}O_4$). The transition heats, ΔQ, were very small to compare with KDP or ADP.

Four types of isotopes, ^{85}Rb-, ^{87}Rb-, ^{64}Zn-, and ^{68}Zn-enriched (independently) Rb_2ZnCl_4 were fabricated as follows: $^{85}RbCl$ (Lot No. 164201), $^{87}RbCl$ (Lot No. 190101), ^{64}ZnO (Lot No. 114901), and ^{68}ZnO (Lot No. 217801) were supplied by the Oak Ridge National Laboratory. 0.01 N hydrochloric acid was added to ZnO powders to get $ZnCl_2$ aqueous solutions. Adding stoichiometric RbCl to the $ZnCl_2$-aqueous solutions, and evaporating excess water, we obtained four types of $^{85}Rb_2ZnCl_4$ (sample A1), $^{87}Rb_2ZnCl_4$ (sample A2), $Rb_2{}^{64}ZnCl_4$ (sample B1), and $Rb_2{}^{68}ZnCl_4$ (sample B2), of which isotope contents are given in Table II. In A_1 and A_2 (Rb isotopes enriched), we used natural ZnO for matching material, for which (natural) Zn isotope contents are also given in Table II. Also, we used natural

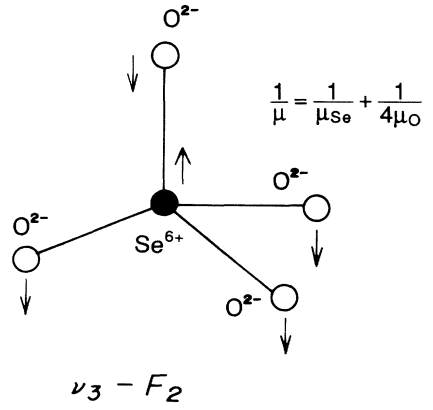

FIG. 7. The ν_3-F_2 vibration mode in SeO_4^{2-}. Se and the four O move in opposite directions.

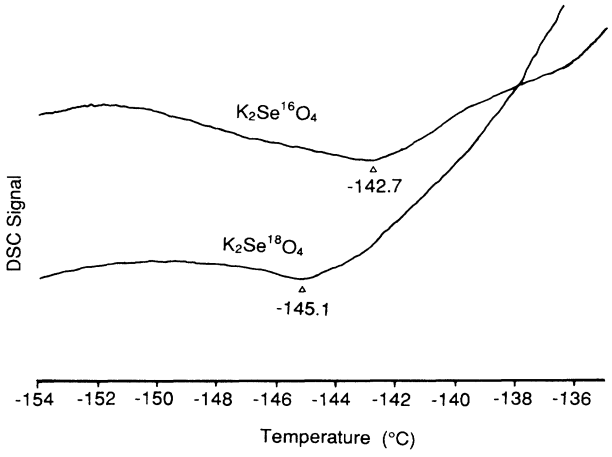

FIG. 8. The DSC signals of $K_2Se^{18}O_4$ and $K_2Se^{16}O_4$ (reference) for heating procedure. Heavy ^{18}O-enriched crystals show about 2.4 °C lower transition temperature (defined from the peaks in the DSC signal). These data were measured with Mettler model DSC-30.

RbCl as the matching material for B_1 and B_2 (Zn isotope enriched), of which isotope contents are also given in Table II.

Figure 9 shows the DSC signals of four types of isotope enriched Rb_2ZnCl_4, A_1, A_2, B_1, and B_2, in which the weights measured were 40 mg and the rising rate was 5 °C/min. We defined T_i as the temperature of peak DSC signal. The transition heats, ΔQ, were also very small, the same as K_2SeO_4. Table II gives T_i for those four materials. We see very small Rb and Zn isotope effects on T_i of Rb_2ZnCl_4, compared to the isotope effect in isomorphic K_2SeO_4. This is reasonable since Rb and Zn are much heavier than O or Cl; hence the movements of Rb and Zn may be much smaller than O in K_2SeO_4 or Cl in Rb_2ZnCl_4 at the phase transitions. Moreover, Zn in Rb_2ZnCl_4, and Se in K_2SeO_4 may form the rigid skeletons; only $ZnCl_4^{2-}$ and SeO_4^{2-} rotate incommensurately along with their center of the gravities (Ref. 12). Zn and Se sit at the center of $ZnCl_4^{2-}$ and SeO_4^{2-}, respectively. Zn and Se scarcely move. Thus the weights of Rb and Zn in the eigenvector of the phonon relating to the incommensurate phase transitions may be small. The reason why we did not try to measure Cl isotope effect in Rb_2ZnCl_4 is that isotopes of ^{35}Cl and ^{37}Cl are supplied in the form of NaCl. Abstraction of Cl from NaCl is somewhat troublesome and expensive for us. We tried as a first step to measure the oxygen isotope effect in isomorphic K_2SeO_4 instead of the Cl isotope effect in Rb_2ZnCl_4. It is expected that the Cl isotope effect on Rb_2ZnCl_4 is very near to that of K_2SeO_4 by O, because they are isomorphic.

E. $NaNO_2$ and KNO_3

Representative order-disorder ferroelectric crystals, $NaNO_2$ and KNO_3, are also called molecular crystals, because with heating $NaNO_2$ is decomposed into Na^+ and NO_2^-, and KNO_3 is decomposed into K^+ and NO_3^-. NO_2^- and NO_3^- are ionic molecules; they are called molecular crystals. Also, $NaNO_2$ has an *incommensurate* phase transition at about 165 °C (T_i), followed by a *ferroelectric* phase transition at about 163.5 °C (T_c).[9,10] The incommensurate transition of $NaNO_2$ is believed to be of the *second kind*.[8] The study of the isotope effect in $NaNO_2$ may give two results, the effect on the incommensurate transition and on the ferroelectric transition, simultaneously.

TABLE II. Isotope contents and the incommensurate phase transition temperatures, T_i, of four types of isotope-enriched Rb_2ZnCl_4. T_i was defined as the temperature of the peak DSC signal. Values in [ ] give isotope contents of naturally obtained materials.

	Isotope contents (%)							T_i
Sample	^{85}Rb	^{87}Rb	^{64}Zn	^{66}Zn	^{67}Zn	^{68}Zn	^{70}Zn	(°C)
A_1	99.78	0.22	[48.89	27.81	4.11	18.56	0.62]	29.4
A_2	2.0	98.00	[48.89	27.81	4.11	18.56	0.62]	29.1
B_1	[72.15	27.85]	99.85	0.14	0.01	0.01	0.01	28.2
B_2	[72.15	27.85]	0.41	0.30	0.20	99.09	0.02	28.1

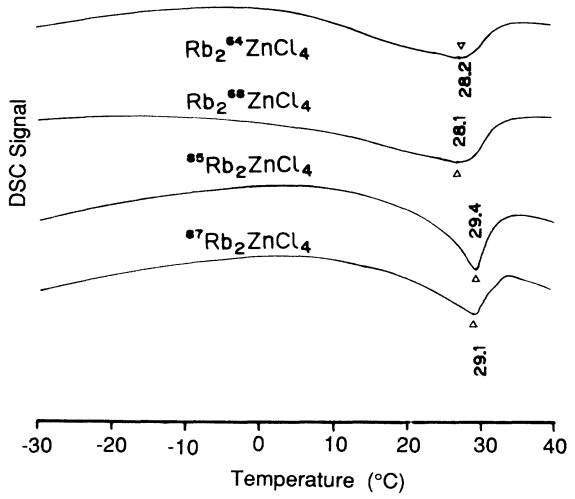

FIG. 9. The DSC signals of four types of isotope-enriched Rb_2ZnCl_4, samples A_1, A_2, B_1, and B_2 (on heating). Isotope contents in them are given in Table II. We see a very weak isotope effect from the DSC signals. This means that Rb and Zn scarcely move at the phase transition. The apparatus was a Rigaku model DSC-8430.

A 99% ^{15}N-enriched $NaNO_2$ was supplied by the Cambridge Isotope Laboratory (Lot No. F-6922). ^{15}N enrichment degree was confirmed by infrared absorption spectroscopy for N—O vibration frequency, to be in good agreement with the nominal (99%) data. Figure 10 shows the infrared absorption data, obtained with a Hitachi IR-260-50. $Na^{15}NO_2$ and natural $NaNO_2$ (with 99.6% ^{14}N used as the reference) were recrystallized by an aqueous solution method. Before the recrystallization, $Na^{15}NO_2$, supplied by Cambridge Isotope Laboratory, was light yellow in color. After the recrystallization, it was completely colorless and transparent. Of course, the reference sample, $Na^{14}NO_2$ was also colorless and trans-

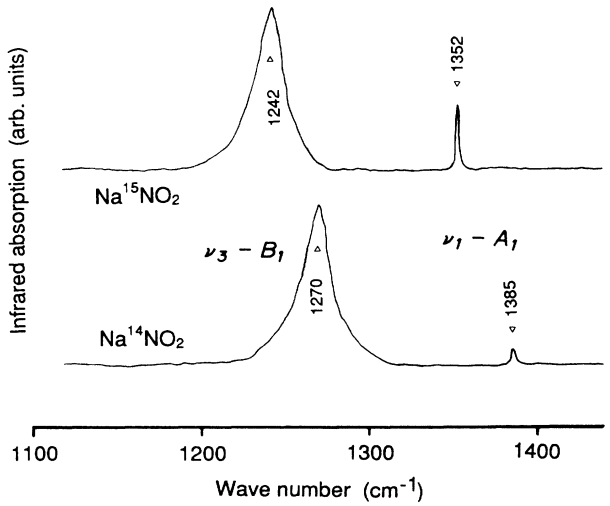

FIG. 10. Infrared absorption spectra of $Na^{15}NO_2$ and $Na^{14}NO_2$. From this figure, we confirmed the ^{15}N isotope degree of enrichment to be equal to the nominal value (more than 95%).

parent. Figure 11(a) shows the DSC signals of Na $^{15}NO_2$ for heating procedures. The weights of the samples for the DSC measurements were 10 mg and the rate of temperature increase was 0.5 °C/min. Also, Fig. 11(b) shows the DSC signal for Na $^{14}NO_2$ (reference), with the same conditions in Na $^{15}NO_2$. We observed a very weak isotope effect; about 0.1 °C higher T_i, and about 0.2 °C higher T_c in *heavy* Na $^{15}NO_2$. The isotope effect in $NaNO_2$ was opposite to all other materials discussed above. However, the experimental error in defining T_i and T_c was about 0.2 °C, being larger than the isotope difference in T_i and T_c, as shown in Fig. 11. We, thus, may say that $NaNO_2$ does not show isotope effects on its T_i and T_c. This means that the phase transitions in $NaNO_2$ are described using the simplest Weiss-type molecular-field model. Rigid NO_2^- molecule has a large *permanent* dipole moment that is unchanged by N-isotope substitution. The phase transitions are presumed to be due to the dipole-dipole interaction of the permanent dipoles on the rigid NO_2^- ionic molecules. The Curie temperature, T_c, in the Weiss theory is given as

$$T_c = N\beta p^2/k_B \ , \tag{4}$$

where N is the number of the dipoles in unit volume, p is the microscopic permanent dipole moment per unit cell of the crystal, k_B is the Boltzmann constant, and β is the coupling coefficient between the dipole moments. Assuming that p has no isotope effect (which means that the short-range force constant between N and O in NO_2^- is not affected by isotope replacing) in $NaNO_2$, we can explain the existence of a null isotope effect in $NaNO_2$. In contrast to $NaNO_2$, the ionic PO_4^{3-} molecule in KDP does not have a permanent dipole moment when decomposed. The microscopic electric dipole appears only in the crystalline state. The different situations in $NaNO_2$ and KDP may be essential for their phase transitions. We observed a very weak but inverse isotope effect in $NaNO_2$. The crystal with light N isotope shows about 0.1–0.2 °C lower T_i and T_c. The lower T_i and T_c in light Na $^{14}NO_2$, if the observed isotope effect is real, may be due to the stronger thermal fluctuations from light ^{14}N. NO_2 that contains light isotope will show, according to classical theory, larger thermal fluctuations than NO_2 that contains heavy isotope; the dipole-dipole interaction in $NaNO_2$ must be reduced in the light-isotope enriched crystal than in the heavy-isotope enriched one.

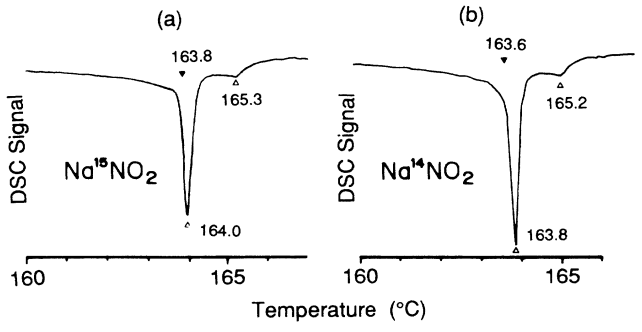

FIG. 11. The DSC signals of Na $^{15}NO_2$ (a) and Na $^{14}NO_2$ [(b); reference] for heating procedure. Very weak isotope effects (0.1–0.2 °C higher T_c and T_i in heavy ^{15}N-enriched crystal) were observed. Temperatures denoted by Δ are the peak temperatures of the DSC signal at the ferroelectric phase transition. The apparatus was a Seiko model DSC-200.

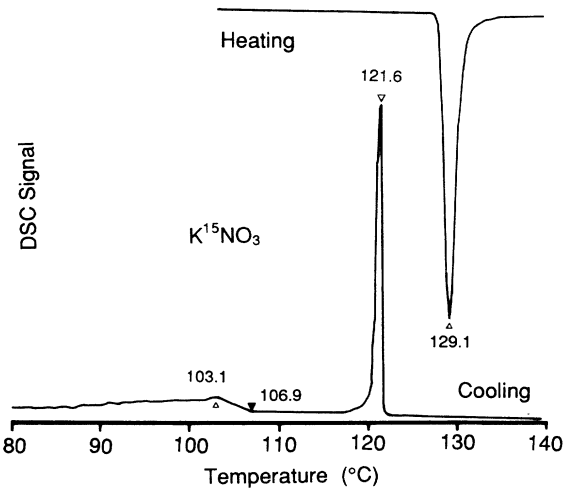

FIG. 12. DSC signals of K $^{15}NO_3$, both for heating and cooling procedures. The apparatus for KNO_3 was a Seiko model DSC-200.

97.8% ^{15}N-enriched KNO_3 was supplied by Shoko Co. (Lot No. 05090). The enrichment degree was confirmed by infrared spectroscopy to be in good agreement with the nominal data. The K $^{15}NO_3$ and natural K $^{14}NO_3$ (used as a reference) were separately recrystallized using an aqueous solution method. Figure 12 shows the DSC signals of K $^{15}NO_3$ both for heating and cooling pro-

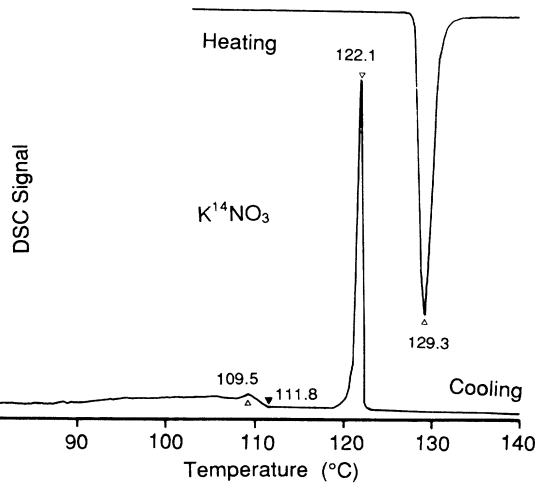

FIG. 13. DSC signals of K $^{14}NO_3$ (reference), both for heating and cooling procedures. In the cooling procedure, the heavy material (K $^{15}NO_3$) shows about a 5 °C lower phase transition temperature in the second transition than the light material (KN $^{14}NO_3$).

cedures. The masses of the samples for the DSC measurement was about 2 mg and the temperature changing rate was 5 °C/min. Also, Fig. 13 shows the DSC signals for light (reference) $K\,^{14}NO_3$, with the same conditions in $K\,^{15}NO_3$. For heating, heavy $K\,^{15}NO_3$ showed about 0.2 °C lower $T_{c(+)}$ than light KNO_3. For cooling procedure, KNO_3 shows two successive transitions. The first (higher) transition temperature, $T_{c1(-)}$, of heavy $K\,^{15}NO_3$ was about 0.5 °C lower than light KNO_3. Also, heavy $K\,^{15}NO_3$ showed about 6 °C lower second (lower) transition temperature, $T_{c2(-)}$, than light KNO_3. The reproducibility of the transition temperatures is within 0.3 °C. The result is very interesting in comparison to the data of $NaNO_2$. KNO_3 will be decomposed into K and NO_3^- by heating. However, KO_3^- is a flat triangle *without* a permanent dipole. Therefore, the situation in KNO_3 is similar to KDP for the origin of the microscopic dipole, and may be opposite to $NaNO_2$ with the permanent dipoles. The isotope effect in KNO_3, which was somewhat different from $NaNO_2$, may be reasonable. The relative ΔQ for two procedures (temperature increasing and decreasing) are, within experimental error, equal for two materials.

III. SUMMARY

The isotope effects, for atoms other than hydrogen, on several types of the structural phase transitions have been measured. Materials studied were $\underline{Li}TaO_3$, $Pb\underline{Zr}O_3$, $\underline{K}H_2\underline{P}O_4$ (KDP), $\underline{N}H_4H_2PO_4$ (ADP), $K_2\underline{Se}O_4$, $\underline{Rb}_2\underline{Zn}CL_4$, $Na\underline{N}O_2$, and $K\underline{N}O_3$. Underlined elements are the isotope replaced elements in our experiments. Those materials are representative crystals for zone-center phonon-freezing-type ferroelectrics ($LiTaO_3$), zone-boundary phonon-freezing-type antiferroelectrics ($PbZrO_3$), ferroelectrics with hydrogen bonds (KDP), antiferroelectrics with hydrogen bonds (ADP), incommensurate-type phase transition materials of the first kind (both K_2SeO_4 and Rb_2ZnCl_4), incommensurate-type phase transition material of the second kind ($NaNO_2$), and ionic molecular ferroelectrics (KNO_3). Moreover, $NaNO_2$ shows a representative order-disorder ferroelectric phase transition just below its incommensurate-type phase transition temperature, T_i. The experimental results are summarized in Table III.

The important result is that when *light* isotopes are substituted, in most of the crystals, the phase transitions

TABLE III. Summary of the results. The * in the isotope (%) means materials with naturally obtained isotopes. Materials are listed up from light isotope-enriched one to heavy isotope-enriched one. Transition-temperature shifts are defined as the difference between the transition temperature of light isotope-enriched crystal and the *heavy* isotope-enriched one, for respective crystals. The negative value of the shift means the lower T_c in heavy isotope-enriched crystal than in light isotope-enriched one. The last column in the table shows the relative transition heat (ΔQ) with respect to the reference materials (with isotopes naturally obtained). For $NaNO_2$, we could only get total transition heat over two transitions, T_i and T_c. Also, for KNO_3, we only obtained total ΔQ for cooling procedure with two transitions, $T_{c1(-)}$ and $T_{c2(-)}$.

Material	Enriched isotope Isotope (%)	Transition Temperature (°C)	Shift (°C)	Transition heat ΔQ
$^6LiTaO_3$	^{6}Li 99.16	$T_c=667.5$	*	1.2
$^7LiTaO_3$	^{7}Li 99.99	655.9	−11.6	1.0
$Pb\,^{90}ZrO_3$	^{90}Zr 99.36	$T_n=234$	*	1.0
$Pb\,^{94}ZrO_3$	^{94}Zr 98.58	230	−4	1.0
KH_2PO_4	*	$T_c=-146.3$	*	1.0
$^{41}KH_2PO_4$	^{41}K 98.88	−146.8	−0.5	1.2
$KH_2P\,^{18}O_4$	^{18}O 98.8	−147.3	−1.0	1.2
$NH_4H_2PO_4$	*	$T_n=-122.0$	*	1.0
$^{15}NH_4H_2PO_4$	^{15}N 99	−123.2	−1.2	0.98
K_2SeO_4	*	$T_i=-142.7$	*	1.0
$K_2Se\,^{18}O_4$	^{18}O >95	−145.1	−2.4	0.95
$^{85}Rb_2ZnCl_4$	^{85}Rb 99.78	$T_i=29.4$	*	1.0
$^{87}Rb_2ZnCl_4$	^{87}Rb 98.0	29.1	−0.3	1.0
$Rb_2\,^{64}ZnCl_4$	^{64}Zn 99.85	28.2	*	1.0
$Rb_2\,^{68}ZnCl_4$	^{68}Zn 99.09	28.1	−0.1	1.0
$NaNO_2$	*	$T_i=165.2$	*	1.0
		$T_c=163.8$	*	
$Na\,^{15}NO_2$	^{15}N 99	$T_i=165.3$	+0.1	0.96
		$T_c=164.0$	+0.2	
KNO_3	*	$T_{c(+)}=129.3$	*	1.0
		$T_{c1(-)}=122.1$	*	1.0
		$T_{c2(-)}=109.5$	*	
$K\,^{15}NO_3$	^{15}N 97.8	$T_{c(+)}=129.1$	−0.2	1.0
		$T_{c1(-)}=121.6$	−0.5	1.0
		$T_{c2(-)}=103.1$	−6.4	

show *higher* transition temperatures than when heavy isotopes are substituted. The exceptions are Rb_2ZnCl_4 and $NaNO_2$. In Rb_2ZnCl_4, Rb and Zn are presumed not to shift at the incommensurate-type-phase transition; hence neither Rb nor Zn show an isotope effect.

In $NaNO_2$, the permanent dipole of rigid NO_2^- ion with permanent dipole is the origin of the dipole-dipole interaction that stimulates the phase transition. From the observed N-isotope effect, we see that the dipole moment is not affected by the N-isotope substitution. $NaNO_2$ therefore shows a pure Weiss-type order-disorder phase transition. Other materials that do not possess a permanent dipole moment when decomposed show the isotope effects of varying degree, with the same trend as the previously reported Ba and Ti isotope effects in $BaTiO_3$.[2] Thus, the isotope effects on the structural phase transitions obtained here and preceding paper are essential for their phase transitions.

In future works, we will study isotope effects for *ferroelastic* phase transitions. It seems to be very important to study isotope effects for the ferroelastic transitions (due to acoustic-phonon freezing) for comparison with ferroelectric transitions (due to transverse optical phonon freezing) which have been the focus of this paper.

ACKNOWLEDGMENTS

One of the authors (T.H.) is very grateful to Dr. H. Yajima of the Optical Information Section, the Electrotechnical Laboratory, for his encouragement, and another author (K.O.) is also very grateful to Dr. H. Unoki of Superconducting Material Section, the Electrotechnical Laboratory, for his encouragement. Thanks are also due to Professor T. Sakudo, Tsukuba University, for useful discussions.

[1]R. Blinc, J. Phys. Chem. Solids **13**, 204 (1960).
[2]T. Hidaka and K. Oka, Phys. Rev. B **35**, 8502 (1987).
[3]B. T. Matthias and J. P. Remeika, Phys. Rev. **76**, 1886 (1949).
[4]E. Sawaguchi, M. Maniwa, and S. Hoshino, Phys. Rev. **83**, 1078 (1951).
[5]G. A. Samara, Phys. Rev. Lett. **27**, 103 (1971).
[6]H. Terauchi, H. Takenaka, and T. Shimooka, J. Phys. Soc. Jpn. **39**, 435 (1975).
[7]K. Gesi and M. Iizumi, J. Phys. Soc. Jpn. **46**, 697 (1979).
[8]Y. Ishibashi, Ferroelectrics **35**, 111 (1981).
[9]S. Sawada, S. Nomura, S. Fujii, and Y. Yoshida, Phys. Rev. Lett. **1**, 320 (1958).
[10]S. Tanisaki, J. Phys. Soc. Jpn. **16**, 579 (1961).
[11]S. Sawada, S. Momura, and S. Fujii, J. Phys. Soc. Jpn. **13**, 1549 (1958).
[12]N. Yamada and T. Ikeda, J. Phys. Soc. Jpn. **53**, 2555 (1984).
[13]M. I. Pope and M. D. Judd, *Differential Thermal Analysis* (Hyden & Son Ltd., London, 1977), p. 102.
[14]S. S. Todd and R. E. Lorenson, J. Am. Chem. Soc. **74**, 544 (1952).
[15]A. M. Glass, Phys. Rev. **172**, 564 (1968).
[16]G. Shirane and A. Takeda, J. Phys. Soc. Jpn. **7**, 1 (1952).
[17]S. Hoshino, K. Vedam, Y. Okaya, and R. Pepinsky, Phys. Rev. **112**, 405 (1958).